

# HIERARCHICAL FILTERING WITH ONLINE LEARNED PRIORS FOR ECG DENOISING

Timur Locher, Guy Revach, Nir Shlezinger, Ruud J. G. van Sloun, and Rik Vullings

## ABSTRACT

Electrocardiographic signals (ECG) are used in many healthcare applications, including at-home monitoring of vital signs. These applications often rely on wearable technology and provide low quality ECG signals. Although many methods have been proposed for denoising the ECG to boost its quality and enable clinical interpretation, these methods typically fall short for ECG data obtained with wearable technology, because of either their limited tolerance to noise or their limited flexibility to capture ECG dynamics. This paper presents HKF, a hierarchical Kalman filtering method, that leverages a patient-specific learned structured prior of the ECG signal, and integrates it into a state space model to yield filters that capture both intra- and inter-heartbeat dynamics. HKF is demonstrated to outperform previously proposed methods such as the model-based Kalman filter and data-driven autoencoders, in ECG denoising task in terms of mean-squared error, making it a suitable candidate for application in extramural healthcare settings.

**Index Terms**— ECG denoising, Kalman filter.

## 1. INTRODUCTION

In the pursuit to halt the increase in healthcare costs and create a sustainable healthcare system, progressively more patients should be monitored outside the hospital environment. In recent years, various technologies have emerged for remote and ambulatory monitoring of vital signs, including wearable electrocardiography (ECG) monitoring devices [1, 2]. The ECG reflects the electrical activity of the heart and is considered one of the most important and informative monitoring modalities, which reveals information about cardiac function and possible pathologies.

Compared with in-hospital monitoring, at-home ECG monitoring comes at the expense of signal quality, e.g., electrodes incorporated in garments, that are used for recording, generally provide noisier signals and with more artifacts than the adhesive electrodes typically used in the hospital [3]. While some of these noises and artifacts can be suppressed by

simple filtering, due to the partial overlap of signal and noise bandwidths, such filtering can only help to some extent [4].

Dedicated ECG denoising strategies include exploitation of the quasi-periodicity of such signals through averaging the ECG of multiple heartbeats [5]. This leads to increased Signal to Noise Ratio (SNR) but can obscure possibly relevant physiological dynamics [5]. An alternative approach models the ECG dynamics as a state space (SS) model, upon which denoising is applied via the Kalman filter (KF) and its variants [5–7]. These methods model the ECG as a sequence of Gaussian kernels or a weighted average of the ECG of previous heartbeats and do not effectively capture strong dynamics within the heartbeat. SS models for ECG were also adopted in [8–12] but these do not effectively capture the quasi-periodicity of the ECG between heartbeats, potentially limiting their performance in denoising the ECG.

In this work we propose HKF, a hierarchical Kalman filtering method for ECG denoising, that increases the quality of the signal without obscuring dynamic changes that could be related to relevant pathophysiology. Our HKF is designed based on our proposed hierarchical SS model that describes the ECG signal dynamics within a heartbeat and between consecutive heartbeats. More specifically, HKF comprises of an online learned structured evolution prior for a single heartbeat; a Rauch-Tung-Striebel (RTS) intra-heartbeat smoother [13] that leverages this prior; and an inter-heartbeat KF [14] for denoising over multiple heartbeats. HKF does not need to be pre-trained in a supervised manner, and is patient-adaptive due to its online covariance estimation and its learned structured evolution prior, while retaining the interpretable nature of the KF. These properties make it appealing for medical and healthcare applications that require a high level of confidence and trustworthiness.

The remainder of this paper is organized as follows: Section 2 formulates the task and describes the hierarchical SS model; Section 3 details the proposed HKF; and Section 4 presents our empirical study, where we show that HKF outperforms model-based and data-driven benchmarks.

## 2. TASK FORMULATION AND SYSTEM MODEL

We start by modeling the activity of the heart as a *hidden* ground truth stochastic process.  $z_t$ . The process is observed by placing multiple electrodes over the human body, here denoted as  $m$  channels, and recording the electrical activity. The features of this recording, e.g., ECG shape, amplitude, noise, and other artifacts, depend on the electrode and its place-

T. Locher and G. Revach are with the Institute for Signal and Information Processing (ISI), D-ITET, ETH Zürich, Switzerland (e-mail: tilocher@student.ethz.ch, grevach@ethz.ch). N. Shlezinger is with the School of ECE, Ben-Gurion University of the Negev, Beer Sheva, Israel (e-mail: nirshl@bgu.ac.il). R. J. G. van Sloun and R. Vullings are with the EE Dpt., Eindhoven University of Technology, The Netherlands, (e-mail: {r.j.g.v.sloun; r.vullings}@tue.nl). We thank Hans-Andrea Loeliger for helpful discussions, and Mehdi Bakka for helping with the empirical evaluation.

ment on the body. We denote the *noiseless* multi-channel recorded electrical activity as  $\mathbf{x}_t \in \mathbb{R}^m$ , and the noisy version as  $\mathbf{y}_t \in \mathbb{R}^m$ . The ECG denoising task is hereby defined as the reconstruction of the  $m$  clean channels,  $\mathbf{x}_t \in \mathbb{R}^m$  from their corresponding past and current noisy observations,  $\{\mathbf{y}_i\}_{i=1}^t$ , by designing a mapping  $\Psi^*$  that minimizes a cost function. A natural loss function is the mean-squared error (MSE):

$$\Psi : \{\mathbf{y}_i\}_{i=1}^t \mapsto \hat{\mathbf{x}}_{t|t}, \quad \Psi^* = \arg \min \mathbb{E} \|\hat{\mathbf{x}}_{t|t} - \mathbf{x}_t\|^2. \quad (1)$$

The relationship between  $\mathbf{x}_t \in \mathbb{R}^m$  and  $\mathbf{y}_t \in \mathbb{R}^m$  correspond to a dynamical system. A canonical way to model dynamical systems in discrete-time is by using SS models [15]. These models blend well with numerous filtering and smoothing techniques. To exploit the periodicity in the ECG signal, we model its dynamics using a *hierarchical* SS model, which is inspired by the decimated components decomposition used to represent periodic systems and cyclostationary signals [16] and as multivariate (tensor) stationary ones. Accordingly, we divide the signal, into periodic segments of length  $T$ , where each such segment stands for a single heartbeat (HB). The dynamics within a single HB are described using an *intra*-HB (internal) SS model, while the dynamics between two consecutive heartbeats are modeled using an *inter*-HB (external) SS model, as detailed next.

For a given HB with index  $\tau$ , we model the dynamics within a single HB with an *intra*-HB SS model. For each time within a single HB  $t \in \{1, \dots, T\} \triangleq \mathcal{T}$ , i.e., the length of a period, the model is given by

$$\mathbf{x}_{\tau,t} = \mathbf{f}_t(\mathbf{x}_{\tau,t-1}) + \mathbf{e}_{\tau,t}, \quad \mathbf{e}_{\tau,t} \sim \mathcal{N}(0, \mathbf{Q}_t), \quad (2a)$$

$$\mathbf{y}_{\tau,t} = \mathbf{x}_{\tau,t} + \mathbf{v}_{\tau,t}, \quad \mathbf{v}_{\tau,t} \sim \mathcal{N}(0, \mathbf{R}_t). \quad (2b)$$

Here,  $\mathbf{f}_t(\cdot)$  is the *intra* evolution prior function that is assumed to be a point-wise vector mapping, but unknown and highly patient-specific;  $\mathbf{Q}_t$  and  $\mathbf{R}_t$  are the *intra* evolution and observation covariance matrices of a Gaussian distribution, which are also assumed to be unknown. In Section 3 we show how a *prior* representation for  $\mathbf{f}_t(\cdot)$  can be learned online with the covariance matrices. For simplicity of description, we don't incorporate the ground truth heart activity into our model but rather model the correlation between channels using the process covariance matrix  $\mathbf{Q}_t$ .

The evolution between two consecutive HBs with indices  $\tau - 1$  and  $\tau$  is described using the following *inter*-HB SS model:

$$\mathbf{x}_{\tau,t} = \mathcal{F}(\mathbf{x}_{\tau-1,t}) + \boldsymbol{\epsilon}_{\tau,t}, \quad \boldsymbol{\epsilon}_{\tau,t} \sim \mathcal{N}(0, \mathbf{Q}_{\tau,t}), \quad (3a)$$

$$\mathbf{y}_{\tau,t} = \mathbf{x}_{\tau,t} + \boldsymbol{\nu}_{\tau,t}, \quad \boldsymbol{\nu}_{\tau,t} \sim \mathcal{N}(0, \mathbf{R}_{\tau,t}). \quad (3b)$$

Here, unlike the intra-state evolution, we assume that due to periodicity, two consecutive HBs look alike, setting the inter-state evolution function  $\mathcal{F}(\cdot)$  to be identity  $\mathcal{F}(\cdot) = \mathbf{I}_m$ . The inter evolution and observation covariance matrices,  $\mathbf{Q}_{\tau}$  and  $\mathbf{R}_{\tau}$  respectively, are assumed to be unknown and have to be

learned within the filtering process. To finalize the hierarchical model, we denote the  $\tau$ th HB and its noisy observation with  $\mathcal{X}_{\tau}$  and  $\mathcal{Y}_{\tau}$ , namely,

$$\mathcal{X}_{\tau} = [\mathbf{x}_{\tau,1}, \dots, \mathbf{x}_{\tau,T}] \in \mathbb{R}^{m \times T}, \quad (4a)$$

$$\mathcal{Y}_{\tau} = [\mathbf{y}_{\tau,1}, \dots, \mathbf{y}_{\tau,T}] \in \mathbb{R}^{m \times T}. \quad (4b)$$

### 3. HIERARCHICAL KALMAN FILTERING

Our customly designed HKF exploits the proposed hierarchical SS model to perform a patient-dependent ECG denoising. The operation of HKF is divided into two main steps:

1. A warm-up *online learning phase* where it learns the patient-dependent characteristics of the intra HB modeling of its ECG signal (2), in an *unsupervised* manner. The learning phase of HKF, detailed in Subsection 3.1, estimates the *prior* signal evolution model using a Taylor least squares (LS) approximation, and learns the missing covariances using expectation-maximization (EM) [17].
2. A *processing phase* in which every HB  $\mathcal{X}_{\tau}$  is denoised in two steps, carried out efficiently in a recursive way, by exploiting all new and previous information. Namely,

- (a) The new observation  $\mathcal{Y}_{\tau}$  is smoothed in a stand-alone manner using the RTS smoother [13, 18] on top of our intra-HB SS model, and given the learned prior to get an estimate  $\hat{\mathcal{X}}_{\tau}$  (see Subsection 3.2)

$$\mathcal{Y}_{\tau} \mapsto \hat{\mathcal{X}}_{\tau} = [\hat{\mathbf{x}}_{\tau,1|T}, \dots, \hat{\mathbf{x}}_{\tau,T|T}] \in \mathbb{R}^{m \times T} \quad (5)$$

- (b) We use a KF with adaptive covariance estimation to fuse the newly improved  $\hat{\mathcal{X}}_{\tau}$  with the previous *posterior* estimate to get a denoised HB (see Subsection 3.3)

$$\hat{\mathcal{X}}_{\tau}, \hat{\mathcal{X}}_{\tau-1|\tau-1} \mapsto \hat{\mathcal{X}}_{\tau|\tau} = [\hat{\mathbf{x}}_{\tau|\tau,1|T}, \dots, \hat{\mathbf{x}}_{\tau|\tau,T|T}] \quad (6)$$

#### 3.1. Learning the SS Model of a Single Heartbeat

The learning phase of HKF estimates the missing SS parameters in (2), i.e.,  $\mathbf{f}_t(\cdot)$  and the noise covariances  $\mathbf{Q}_t$ , and  $\mathbf{R}_t$ .

**Estimating  $\mathbf{f}_t(\cdot)$ :** There is an inherent difficulty in modelling the evolution of such physiological processes analytically. The variability of the signal between patients makes it a challenging task, and limits the ability to learn it offline from data corresponding to other patients. To tackle this, we adopt a mathematically solid evolution model based on the Taylor approximation, which has few parameters and can be trained online using patient-specific observations. We write the state evolution as a time-dependent finite Taylor expansion:

$$d\mathbf{x}_t \triangleq \mathbf{x}_{t+\Delta t} - \mathbf{x}_t = \sum_{k=1}^K \frac{d\mathbf{x}_t}{dt^k} \cdot \frac{\Delta t^k}{k!}, \quad K \rightarrow \infty. \quad (7)$$

Based on (7), we model the state difference in time step  $t$  as a noisy linear combination of *basis* functions  $\Phi^\top$ , with the unknown time-dependent parameters vector  $\Theta_t$  corresponding to the high-order signal derivatives (up to order  $K$ ):

$$d\mathbf{x}_t \approx \Phi^\top \cdot \Theta_t, \quad \Phi^\top = \left( \Delta t, \frac{\Delta t^2}{2}, \dots, \frac{\Delta t^K}{K!} \right). \quad (8)$$

We thus use the following parametric model for  $\mathbf{f}_t(\cdot)$

$$\mathbf{f}_t(\mathbf{x}_{t-1}) = \mathbf{x}_{t-1} + \Phi^\top \cdot \Theta_t. \quad (9)$$

The model in (9) provides a simple and structured representation of  $\mathbf{f}_t(\cdot)$ . The learning of its parameters  $\Theta_t$  is a form of linear regression, which can be solved using LS minimization. Specifically, for each time point  $t \in \mathcal{T}$ , we collect observations from multiple HBs,  $\tau = 1, \dots, N$ . By defining the LS in a time-windowed fashion, such that  $w_\ell$  are the window weights<sup>1</sup>, we can exploit time correlations within a HB and get a smoother prior. Since the state is directly observed, as defined in (2b), minimizing the loss using noisy observations is equivalent, and we can learn the representation in a patient-dependent *unsupervised* fashion,

$$\mathcal{L}(t) = \sum_{\tau=1}^N \sum_{\ell=-L_1}^{L_2} w_\ell \cdot \|\hat{d}\mathbf{y}_{\tau,t+\ell} - d\mathbf{y}_{\tau,t+\ell}\|^2. \quad (10)$$

**Estimating  $\mathbf{Q}_t, \mathbf{R}_t$ :** For the noise covariances, we employ the EM method, commonly adopted for such purposes in SS models [19–21]. EM is an iterative<sup>2</sup> method that alternates between the E-step and the M-step. The E-step is a conditional expectation, which here computes posterior second-order moments via the RTS smoother:

$$\mathbf{X}_t^{\text{II}} = \|\hat{\mathbf{x}}_{t|T}\|^2 + \mathbf{P}_{t|T}, \quad \mathbf{X}\mathbf{Y}_{t,t} = \hat{\mathbf{x}}_{t|T}\mathbf{y}_t^\top, \quad \mathbf{Y}_t^{\text{II}} = \|\mathbf{y}_t\|^2, \\ \mathbf{X}\mathbf{X}_{t,t-1} = \hat{\mathbf{x}}_{t|T} \cdot \hat{\mathbf{x}}_{t-1|T} + \mathbf{P}_{t|T} \cdot \mathcal{G}_{t-1}^\top,$$

and the M-step is the maximum likelihood estimation given the outcome of the previous step:

$$\hat{\mathbf{Q}}_t = \frac{1}{\tilde{L}} \cdot \sum_{\ell=-L_1}^{L_2} \tilde{\mathbf{Q}}_{t+\ell}, \quad \tilde{\mathbf{Q}}_t = \mathbf{X}_t^{\text{II}} - 2 \cdot \mathbf{X}\mathbf{X}_{t,t-1} + \mathbf{X}_{t-1}^{\text{II}} \\ \hat{\mathbf{R}} = \frac{1}{\tilde{T}} \cdot \sum_{\tilde{t}=1}^{\tilde{T}} \tilde{\mathbf{R}}_{\tilde{t}}, \quad \tilde{\mathbf{R}}_t = \mathbf{Y}_t^{\text{II}} - 2 \cdot \mathbf{Y}\mathbf{X}_{t,t} + \mathbf{X}_t^{\text{II}}.$$

Here, due the unique shape of the HB, we assume that the process noise is non-intra-HB invariant, therefore averaged in short window with length  $\tilde{L} = L_1 + L_2 + 1$ , while the observation noise is assumed to intra-HB invariant, namely given the short duration, it is assumed to change across larger time-scales, and averaged across the entire HB. To exploit inter-HB correlations we unfold the EM algorithm over multiple HBs.

<sup>1</sup>The window can have any weights, as long as they sum to 1.

<sup>2</sup>For brevity we ignore the iteration index

### 3.2. Smoothing a Single Heartbeat

We employ the RTS smoother [13] to map a block of noisy observations into posterior estimates of the hidden states. The RTS smoother includes a *forward* pass (a KF), and a *backward* pass. The KF is also described in two steps: *prediction*, given by<sup>3</sup>

$$\hat{\mathbf{x}}_{t|t-1} = \mathbf{f}_t(\hat{\mathbf{x}}_{t-1|t-1}), \quad \mathbf{P}_{t|t-1} = \mathbf{P}_{t-1|t-1} + \mathbf{Q}_t, \quad (11a)$$

$$\hat{\mathbf{y}}_{t|t-1} = \hat{\mathbf{x}}_{t|t-1}, \quad \mathbf{S}_t = \mathbf{P}_{t|t-1} + \mathbf{R}_t. \quad (11b)$$

and *update*, given by

$$\hat{\mathbf{x}}_{t|t} = \hat{\mathbf{x}}_{t|t-1} + \mathcal{K}_t \cdot \Delta \mathbf{y}_t, \quad \Delta \mathbf{y}_t = \mathbf{y}_t - \hat{\mathbf{y}}_{t|t-1}, \quad (12a)$$

$$\mathbf{P}_{t|t} = \mathbf{P}_{t|t-1} - \mathcal{K}_t \cdot \mathbf{S}_t \cdot \mathcal{K}_t^\top, \quad \mathcal{K}_t = \mathbf{P}_{t|t-1} \cdot \mathbf{S}_t^{-1}. \quad (12b)$$

The *backward* pass of the RTS smoother is given by

$$\hat{\mathbf{x}}_{t|T} = \hat{\mathbf{x}}_{t|t} + \mathcal{G}_t \cdot \Delta \mathbf{x}_t, \quad \Delta \mathbf{x}_t = \hat{\mathbf{x}}_{t+1|T} - \hat{\mathbf{x}}_{t+1|t}, \quad (13a)$$

$$\mathbf{P}_{t|T} = \mathbf{P}_{t|t} - \mathcal{G}_t \cdot \Delta \mathbf{P}_{t+1} \cdot \mathcal{G}_t, \quad (13b)$$

$$\Delta \mathbf{P}_{t+1} = \mathbf{P}_{t+1|T} - \mathbf{P}_{t+1|t}, \quad \mathcal{G}_t = \mathbf{P}_{t|t} \mathbf{P}_{t+1|t}^{-1}. \quad (13c)$$

### 3.3. Filtering Consecutive Heartbeats

Finally, we harness the temporal dependence between two consecutive HBs  $\tau - 1$  and  $\tau$ , as defined in (3). For each  $t \in \mathcal{T}$  and given the estimated covariance matrices, we apply  $T$  independent (and parallel) KFs. Namely<sup>4</sup>

$$\mathcal{P}_{\tau|\tau-1} = \mathcal{P}_{\tau-1|\tau-1} + \hat{\mathbf{Q}}_\tau, \quad \mathcal{S}_\tau = \mathcal{P}_{\tau|\tau-1} + \hat{\mathbf{R}}_\tau, \quad (14a)$$

$$\mathcal{P}_{\tau|\tau} = \mathcal{P}_{\tau|\tau-1} - \mathcal{K}_\tau \cdot \mathcal{S}_\tau \cdot \mathcal{K}_\tau^\top, \quad \mathcal{K}_\tau = \mathcal{P}_{\tau|\tau-1} \cdot \mathcal{S}_\tau^{-1} \quad (14b)$$

$$\hat{\mathcal{X}}_{\tau|\tau} = \hat{\mathcal{X}}_{\tau-1|\tau-1} + \mathcal{K}_\tau \cdot \left( \hat{\mathcal{X}}_\tau - \hat{\mathcal{X}}_{\tau-1|\tau-1} \right). \quad (14c)$$

To obtain  $\hat{\mathcal{R}}_{\tau,t}$  and  $\hat{\mathcal{Q}}_{\tau,t}$ , we recall that we used the previously *smoothed* vector  $\hat{\mathcal{X}}_\tau$  as the observation vector. We observe the covariance of the following differences in time point  $t \in \mathcal{T}$

$$\hat{\mathcal{X}}_{\tau,t} - \mathcal{X}_{\tau,t} \sim \mathcal{P}_{\tau,t|T} = \hat{\mathcal{R}}_{\tau,t}, \quad \mathcal{X}_{\tau,t} - \mathcal{X}_{\tau-1,t} \sim \mathcal{Q}_{\tau,t} \\ \mathcal{X}_{\tau-1,t} - \hat{\mathcal{X}}_{\tau-1|\tau-1,t} \sim \mathcal{P}_{\tau-1|\tau-1,t}. \quad (15)$$

The maximum likelihood estimation is then given by [22]

$$\hat{\mathcal{Q}}_{\tau,t} = \max \left\{ \left\| \hat{\mathcal{X}}_{\tau,t} - \hat{\mathcal{X}}_{\tau-1|\tau-1,t} \right\|^2 - \mathcal{P}_{\tau-1|\tau-1,t} - \hat{\mathcal{R}}_{\tau,t}, 0 \right\}.$$

For increased robustness we can exploit inter-HB correlations by additional exponential smoothing. The intra-HB correlations can be exploited as well for further smoothness.

<sup>3</sup>For brevity we ignore the inter-HB index  $\tau$ .

<sup>4</sup>For brevity we ignore the intra-HB index  $t$ .

### 3.4. Discussion

The proposed HKF exploits both intra- and inter-HB relations via the proposed SS model and can operate on multi-dimensional data, thereby also exploiting spatial relations across ECG signals recorded with multiple electrodes. Our derivation imposes several simplifications, mainly concerning properties of the process and observation noise covariances, that make HKF analytically tractable and keep computational loads relatively manageable. A natural extension of HKF would be to replace the intra- and inter-HB smoothing and filtering with the recently proposed RTSNet and KalmanNet [23, 24] respectively, yielding a *hybrid* model-based/data-driven ECG denoiser. We anticipate that this extension, which is left for future study, will further improve the performance as it relaxes the simplifications mentioned above and improves upon HKF noise tolerance.

## 4. EMPIRICAL EVALUATION

We empirically evaluate<sup>5</sup> HKF for ECG denoising on two data sets: *PhysioNet* data set [25] where only two channels were available; the proprietary data set considered in [5, 26], where four channels were available. The measurements are corrupted by white Gaussian noise of 0 [dB] Signal to Noise Ratio. To evaluate the individual gains of the two main processing steps in HKF, it is compared with solely intra-HB smoothing (*KS-intra*), and with *inter*-HB KF processing [5] (*KF-inter*). We also use a denoiser data-driven convolutional auto-encoder (AE) following [26, 27]. Here, *AE-intra* denotes only an intra-HB processing using the AE, while *AE-KF* denotes an additional step of *inter*-HB processing using the KF as in [5], on top of the AE. The results presented in Table 1 and Figure 1 show quantitatively and visually that our HKF ECG denoising outperforms its benchmarks, and that it shares the rapid runtime of model-based denoisers.

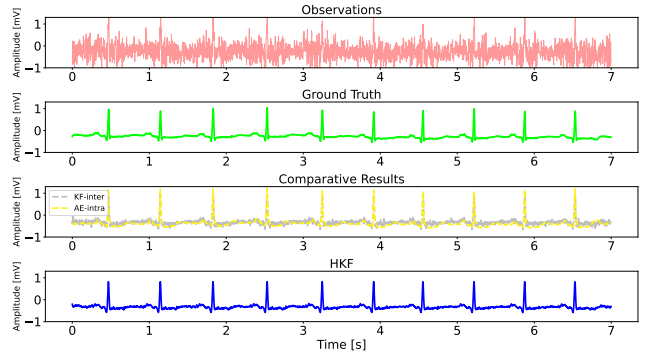
**Table 1:** Empirical evaluation: MSE [dB], Time [msec]

	PhysioNet ( $m = 2$ )		Proprietary ( $m = 4$ )	
	MSE	Time	MSE	Time
<i>KF-inter</i> [5]	-19.36	23.7	-17.95	86.8
<i>KS-intra</i>	-20.24	104.0	-22.20	122.9
<i>AE-intra</i>	-16.10	36.6	-23.63	341.1
<i>AE-KF</i>	-16.11	62	-23.73	434.4
<b>HKF</b>	<b>-23.19</b>	<b>122.8</b>	<b>-25.10</b>	<b>141.5</b>

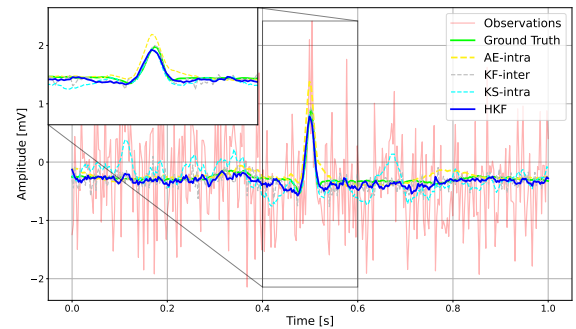
## 5. CONCLUSIONS

We proposed HKF for ECG denoising. We formulate the ECG system model as a hierarchical SS system model, based on which hierarchical Kalman filter (HKF) is designed, combining KF and RTS smoothing with a learned prior. The proposed method does not require supervised pre-training and, due its structured prior, can adapt to patient-specific characteristics in the ECG. HKF is demonstrated to reliably denoise ECG signals while being rapid and interpretable.

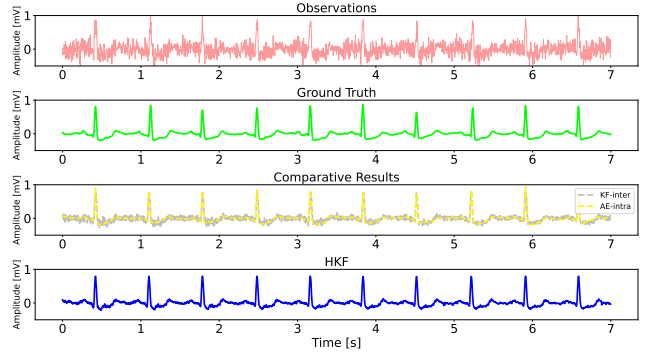
<sup>5</sup>The source code used in our empirical study along with hyperparameters is at [https://github.com/KalmanNet/HKF\\_ICASSP23](https://github.com/KalmanNet/HKF_ICASSP23).



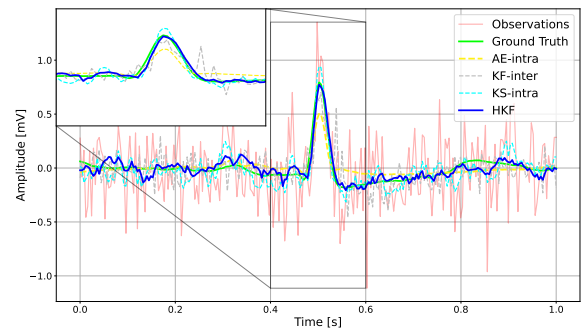
(a) PhysioNet - Multiple



(b) PhysioNet - Single



(c) Proprietary - Multiple



(d) Proprietary - Single

**Fig. 1:** Empirical evaluation

## 6. REFERENCES

- [1] Y. Bai, C. Tompkins, N. Gell, D. Dione, T. Zhang, and W. Byun, "Comprehensive comparison of Apple Watch and Fitbit monitors in a free-living setting," *PLoS One*, vol. 16, no. 5, p. e0251975, 2021.
- [2] F. Sana, E. M. Isselbacher, J. P. Singh, E. K. Heist, B. Pathik, and A. A. Armoundas, "Wearable devices for ambulatory cardiac monitoring: Jacc state-of-the-art review." *Journal of the American College of Cardiology*, vol. 75 13, pp. 1582–1592, 2020.
- [3] A. Gruetzmann, S. Hansen, and J. Müller, "Novel dry electrodes for ECG monitoring," *Physiol. Meas.*, vol. 28, pp. 1375–1390, 2007.
- [4] J. Bailey *et al.*, "Recommendations for standardization and specifications in automated electrocardiography: Bandwidth and digital signal processing," *Circulation*, vol. 81, pp. 730–739, 1990.
- [5] R. Vullings, B. de Vries, and J. W. M. Bergmans, "An adaptive Kalman filter for ECG signal enhancement," *IEEE Trans. Biomed. Eng.*, vol. 58, 2011.
- [6] R. Sameni, M. B. Shamsollahi, C. Jutten, and G. D. Clifford, "A nonlinear bayesian filtering framework for ECG denoising," *IEEE Trans. Biomed. Eng.*, vol. 54, no. 12, pp. 2172–2185, 2007.
- [7] O. Sayadi and M. B. Shamsollahi, "ECG denoising and compression using a modified extended kalman filter structure," *IEEE Trans. Biomed. Eng.*, vol. 55, no. 9, pp. 2240–2248, 2008.
- [8] R. A. Wildhaber, N. Zalmi, M. Jacomet, and H. Loeliger, "Windowed state-space filters for signal detection and separation," *IEEE Trans. Signal Process.*, vol. 66, no. 14, pp. 3768–3783, 2018.
- [9] R. A. Wildhaber, "Localized state space and polynomial filters with applications in electrocardiography," Ph.D. dissertation, ETH Zurich, Zurich, Switzerland, 2019.
- [10] R. A. Wildhaber, E. Ren, F. Waldmann, and H. Loeliger, "Signal analysis using local polynomial approximations," in *EUSIPCO 2020*.
- [11] R. M. Evaristo, A. M. Batista, R. L. Viana, K. C. Iarosz, J. D. Szezech Jr, and M. F. de Godoy, "Mathematical model with autoregressive process for electrocardiogram signals," *Communications in Nonlinear Science and Numerical Simulation*, vol. 57, pp. 415–421, 2018.
- [12] F. Huang, T. Qin, L. Wang, H. Wan, and J. Ren, "An ECG signal prediction method based on ARIMA model and DWT," in *2019 IEEE IAEAC*.
- [13] H. E. Rauch, F. Tung, and C. T. Striebel, "Maximum likelihood estimates of linear dynamic systems," *AIAA Journal*, vol. 3, no. 8, pp. 1445–1450, 1965.
- [14] R. E. Kalman, "A new approach to linear filtering and prediction problems," *Journal of Basic Engineering*, vol. 82, no. 1, pp. 35–45, 1960.
- [15] Y. Bar-Shalom, X. R. Li, and T. Kirubarajan, *Estimation with applications to tracking and navigation: theory algorithms and software*. John Wiley & Sons, 2004.
- [16] G. B. Giannakis, "Cyclostationary signal analysis," in *Digital Signal Processing Handbook*, 1998, vol. 31, pp. 1–17.
- [17] T. K. Moon, "The expectation-maximization algorithm," *IEEE Signal Process. Mag.*, vol. 13, no. 6, 1996.
- [18] S. Särkkä, *Bayesian filtering and smoothing*. Cambridge University Press, 2013, no. 3.
- [19] Z. Ghahramani and G. E. Hinton, "Parameter estimation for linear dynamical systems," University of Toronto, Dept. of CS, Tech. Rep. CRG-TR-96-2, 02 1996.
- [20] J. Dauwels, A. Eckford, S. Korl, and H.-A. Loeliger, "Expectation maximization as message passing-part I: Principles and Gaussian messages," *arXiv preprint arXiv:0910.2832*, 2009.
- [21] Sophocles J. Orfanidis, *Applied Optimum Signal Processing*. Rutgers University, 2018.
- [22] P. De Jong, "The likelihood for a state space model," *Biometrika*, vol. 75, no. 1, pp. 165–169, 1988.
- [23] X. Ni, G. Revach, N. Shlezinger, R. J. G. van Sloun, and Y. C. Eldar, "RTSNet: Deep learning aided Kalman smoothing," in *IEEE ICASSP 2022*.
- [24] G. Revach, N. Shlezinger, X. Ni, A. L. Escoriza, R. J. Van Sloun, and Y. C. Eldar, "KalmanNet: Neural network aided Kalman filtering for partially known dynamics," *IEEE Trans. Signal Process.*, vol. 70, 2022.
- [25] A. L. Goldberger *et al.*, "Physiobank, physiotookit, and physionet: components of a new research resource for complex physiologic signals," *circulation*, vol. 101, no. 23, pp. e215–e220, 2000.
- [26] E. Fotiadou and R. Vullings, "Multi-channel fetal ECG denoising with deep convolutional neural networks," *Frontiers in Pediatrics*, vol. 8, 2020.
- [27] H. Chiang, Y. Hsieh, S. Fu, K. Hung, Y. Tsao, and S. Chien, "Noise reduction in ECG signals using fully convolutional denoising autoencoders," *IEEE Access*, vol. 7, pp. 60 806–60 813, 2019.